Architecture-Induced Phase Immiscibility in a Diblock/Multiblock Copolymer Blend

Richard J. Spontak,*,† Jennifer C. Fung,‡ Michael B. Braunfeld,§ John W. Sedat,§ David A. Agard,§ Arman Ashraf,|| and Steven D. Smith*,||

Department of Materials Science & Engineering, North Carolina State University, Raleigh, North Carolina 27695, Graduate Group in Biophysics and Department of Biophysics & Biochemistry and Howard Hughes Medical Institute, University of California, San Francisco, California 94143, and Corporate Research Division, The Procter & Gamble Company, Cincinnati, Ohio 45239

Received October 24, 1995; Revised Manuscript Received December 27, 1995[⊗]

ABSTRACT: Ordered diblock copolymer blends have recently become the subject of tremendous research interest since they can be used to elucidate the intramicrodomain segregation of blocks differing in length, as well as to identify the molecular and blend parameters yielding phase immiscibility. In this work, we explore the influence of molecular architecture on block copolymer blend miscibility by examining an equimolar mixture of two symmetric styrene (S)/isoprene (I) block copolymers, one an SI diblock and the other an $(SI)_4$ octablock. Their molecular weights are identical, so that the ratio of block lengths is 4:1 SI:$(SI)_4$. While this ratio is expected to yield a single phase in diblock copolymer blends, transmission electron microscopy reveals here that the diblock/multiblock blend is macrophase-separated due to the linear multiblock architecture and midblock conformations of the $(SI)_4$ copolymer. Electron tomography (3D imaging) permits direct visualization of connected SI and $(SI)_4$ microdomains at the SI/$(SI)_4$ interface at relatively high spatial resolution (ca. 3 nm). In addition, the presence of SI molecules in the $(SI)_4$ phase or $(SI)_4$ molecules in the SI phase frustrates SI lamellae, resulting in curved microphase boundaries.

Introduction

Microphase-ordered block copolymers continue to constitute a fascinating, and technologically important, class of materials since they elucidate the factors governing polymer self-assembly and exhibit a wide (and controllable) range of properties.[1−4] While the morphology and properties of a neat block copolymer can be altered[5−7] or refined[8−10] through processing, they are usually tailored for a specific application via chemical synthesis. Another, potentially more effective, route by which to obtain a microphase-ordered polymeric material possessing particular morphological characteristics or properties is through blending at the molecular level. Studies of diblock copolymer/homopolymer blends, for instance, have demonstrated that the addition of a parent homopolymer (hA) to an ordered (usually lamellar) AB copolymer can result in either preferential microstructural swelling,[11,12] a morphological transition,[13−16] or macrophase separation,[14] depending on both the blend volume-fraction composition (Φ_A) and the molecular weight of hA relative to that of the A block of the copolymer (M_{hA}/M_A). In fact, theoretical studies[17] predict that a wide variety of morphologies can be readily accessed through the use of AB/hA blends.

To avoid the complication of hA localization within the host microdomains of such blends, recent efforts have begun to focus more on the use of block copolymer/copolymer, $(AB)_\alpha/(AB)_\beta$, blends as an alternative means to produce microphase-ordered materials with controlled morphologies and properties. While this idea is not new,[18] such blends thus far have expedited the study of (i) morphological transitions between adjacent microphases,[19−21] (ii) intramicrodomain block mixing and conformations,[22−25] and (iii) molecular/blend parameters responsible for either morphological coexistence or phase immiscibility.[23,25−27] According to experimental studies[22,26] and self-consistent field (SCF) predictions,[25] phase immiscibility between two symmetric diblock copolymers (of equal composition) occurs when the ratio of copolymer chain lengths (N_α/N_β, with $N_\alpha > N_\beta$) exceeds a critical value that is dependent on the thermodynamic incompatibility (χN, where χ is the Flory−Huggins interaction parameter) of the longer α copolymer. It is important to recognize at this juncture that the blocks of each diblock copolymer in a binary $(AB)_\alpha/(AB)_\beta$ blend are constrained only at one end, in which case the α and β blocks occupying each microphase in the blend constitute a bidisperse mixture of grafted chains that comprises a two-tier polymer brush[28] (with the long α blocks forcing the short β blocks to reside in a boundary layer adjacent to the highly repulsive microdomain interphase). Phase immiscibility in such blends therefore is the result of a critical difference in copolymer block lengths.

In contrast to diblock copolymers, perfectly alternating linear $(AB)_n$ multiblock copolymers with $n > 1$ (n denotes the number of AB block pairs) consist of 2 single-grafted endblocks and $2(n - 1)$ double-grafted midblocks, each of which is capable of adopting a bridged or looped conformation (see Figure 1). Previous experimental[29−32] and theoretical[33] studies have demonstrated that, at constant χ, the microstructural dimensions of symmetric $(AB)_n$ copolymers are dependent on molecular factors such as n and N, as well as on conformational factors such as q, where q denotes the fraction of bridged midblocks present in the lamellar microstructure. Related studies[34] have also shown that the linear multiblock architecture and the existence of bridged/looped midblock conformations effect a reduction in the miscibility of $(AB)_n$/hA blends. While blends composed of hA and an AB diblock copolymer ($M_{hA}/M_A \approx 0.5$) are miscible at $\Phi_A = 0.66$, for example, identical blends with an $(AB)_n$ copolymer ($2 \leq n \leq 4$) are not.

* Authors to whom correspondence should be addressed.
† North Carolina State University.
‡ Graduate Group in Biophysics, University of California.
§ Department of Biophysics & Biochemistry and Howard Hughes Medical Institute, University of California.
|| The Procter & Gamble Co.
⊗ Abstract published in *Advance ACS Abstracts,* February 15, 1996.

0024-9297/96/2229-2850$12.00/0

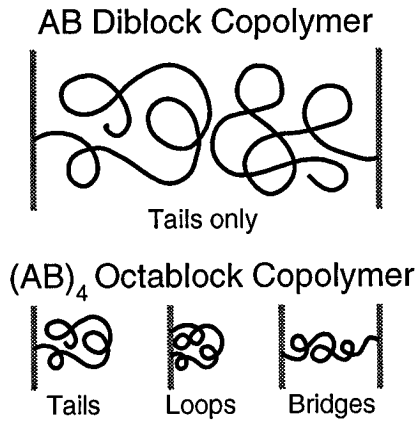

Figure 1. Schematic illustration showing the differences in chain length and conformations of the AB diblock and $(AB)_4$ octablock copolymers examined in this study. While diblock molecules are restricted to one conformation, an octablock molecule may assume any one of 64 conformations, with each of its 6 midblocks adopting either a bridged or looped conformation.

The objective of this work is to examine the phase behavior of an equimolar diblock/multiblock copolymer blend. Conventional and advanced transmission electron microscopy (TEM) techniques, including intermediate-voltage electron microscopic tomography (IVEM-T), are employed here to characterize the blend morphology, so that the effect of copolymer architecture on copolymer/copolymer blend miscibility can be discerned.

Experimental Section

Materials. Two block copolymers composed of styrene (S) and isoprene (I) monomers were synthesized in the presence of *sec*-butyllithium catalyst via living anionic polymerization in cyclohexane at 60 °C. One copolymer was a symmetric (50:50 wt % S/I) SI diblock with $\bar{M}_n = 120\,000$ (60 000 blocks) and $\bar{M}_w/\bar{M}_n \approx 1.05$, while the other was a symmetric $(SI)_4$ octablock with $\bar{M}_n = 120\,000$ (15 000 blocks) and $\bar{M}_w/\bar{M}_n \approx 1.09$. Copolymer compositions and molecular weights/molecular weight distributions were measured by ^{1}H NMR and GPC, respectively, and are described in detail elsewhere.[29] On the basis of small-angle X-ray scattering (SAXS) results,[35] the thermodynamic incompatibility (χN) of the SI copolymer is estimated to be about 86 at its upper glass transition temperature (≈100 °C, from differential scanning calorimetry), indicating that the neat copolymer resides in the intermediate-segregation regime at ambient temperature.

Methods. Equal masses of the two copolymers were dissolved in toluene to produce a 4% (w/v) solution, which, upon complete copolymer dissolution (12 h), was cast into a Teflon mold. To obtain a near-equilibrium blend morphology, solvent was removed slowly over the course of 3 weeks, and the resultant film, measuring ca. 2 mm thick, was heated at 100 °C under low vacuum for 5 h to remove residual solvent. The film was subsequently encapsulated in a glass tube that was first cycled between Ar and vacuum three times and then subjected to 160 °C for 1 week. No gross signs of thermooxidative degradation were evident, and the film readily redissolved in toluene (suggesting that little, if any, cross-linking occurred during heat treatment). The film was trimmed so that its interior (presumably removed from surface artifacts) could be cross-sectioned on a Reichert-Jung Ultracut-S microtome maintained at −100 °C. Sections measuring less than 100 nm thick were subsequently stained with the vapor of 2% OsO_4(aq) for 90 min to enhance electron contrast between the S and I microphases. Specimens employed in electron tomography were coated with a 1% polylysine solution to enhance surface hydrophilicity and then decorated with 30 nm colloidal gold (required as reference markers, as described in the following).

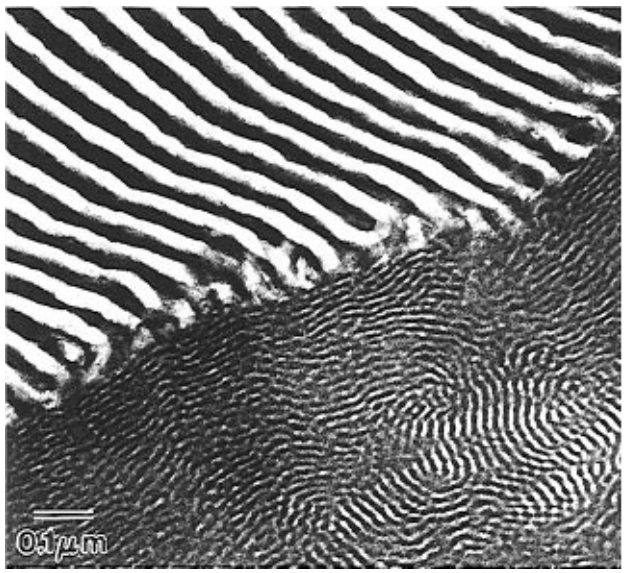

Figure 2. Transmission electron micrograph of an equimolar SI/$(SI)_4$ blend, revealing that the blend, is immiscible and that the SI and $(SI)_4$ phases (large and small lamellae, respectively) are separated by relatively sharp interfaces.

Conventional TEM micrographs were obtained on a Zeiss EM902 electron spectroscopic microscope operated at 80 kV and $\Delta E = 50$ eV. For IVEM-T, digital images of an SI/$(SI)_4$ interface were collected on a 12 bits/pixel cooled slow-scan CCD camera in a Philips 430 electron microscope operated at 200 kV. The image resolution was 1.7 nm/pixel. Forty-nine 480 × 480 pixel images were collected from a single specimen at tilt angles (θ) ranging from −60° to 60° in 2.5° increments along a single-tilt axis. Of these, 43 images were mass-normalized (i.e., converted from image intensity to mass density) and then aligned (by least-squares minimization) by using eight colloidal gold beads as fiducial markers. Upon satisfactory alignment, as discerned from the mean error in bead position (σ), the image stack was reconstructed according to the *r*-weighted (filtered) back-projection method[21,36−38] using the EMCAT reconstruction software package.[39] The resultant 3D volume element was displayed and analyzed in the PRIISM image graphics package,[40] where it was sliced along orthogonal directions to facilitate parallel and perpendicular viewing of the interface.

Results and Discussion

Presented in Figure 2 is a conventional TEM micrograph of the macroscopic interface separating the SI and $(SI)_4$ phases, clearly revealing that these two copolymers, while of equal molecular weight and composition, are immiscible. The ratio of block lengths between these two copolymers is 4:1 SI:$(SI)_4$, which is less than that needed for immiscibility in a symmetric blend of two diblock copolymers (about 5.6:1, as discerned from the predictions provided in ref 33 evaluated at $\chi N_\alpha = 80$, where α denotes the longer copolymer). According to the SAXS and TEM data of Hashimoto *et al.*[26] and Kane *et al.*,[41] ordered diblock copolymers remain fully miscible for $\bar{M}_n$ ratios less than 5.2:1. Thus, it is reasonable to attribute the copolymer immiscibility evident in Figure 2 to the molecular architecture of the $(SI)_4$ molecules, each of which contains six midblocks that are capable of adopting either a bridged or a looped conformation. Since either conformation halves the lateral extension of a midblock along the lamellar normal (relative to that of an endblock), the ratio between SI endblocks and $(SI)_4$ midblocks is effectively 8:1, which exceeds the experimental and predicted miscibility limits for two diblock copolymers.

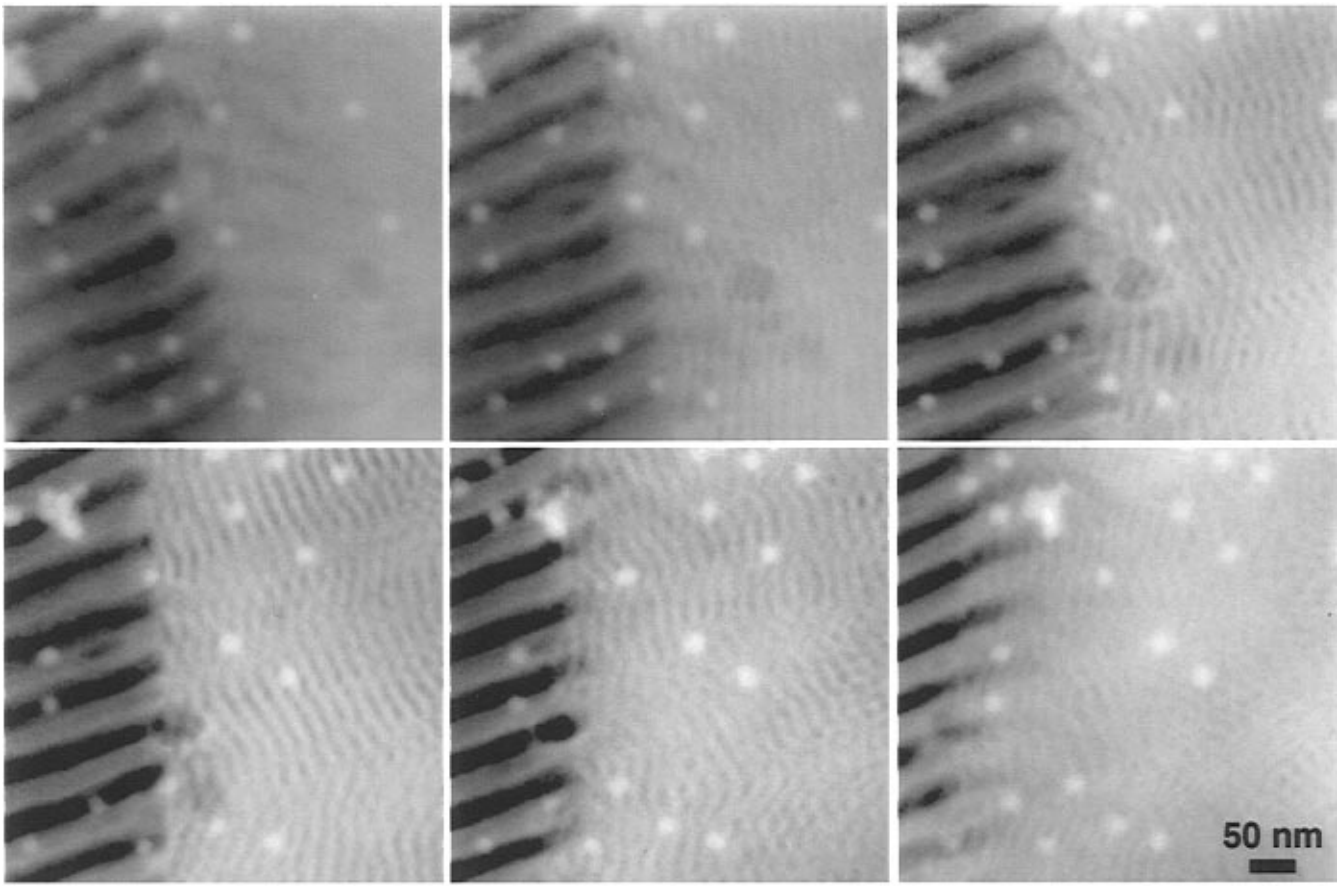

Figure 3. Series of digital micrographs of the SI/$(SI)_4$ interface at tilt angles ranging from −45° to 30° in 15° increments (from left to right and top to bottom) along a single-tilt axis. The images are contrast-reversed, mass-normalized, and aligned to facilitate viewing. The bright dots correspond to the colloidal gold beads used during image alignment.

Microdomain periodicities of the SI and $(SI)_4$ phases measured from micrographs such as the one shown in Figure 2 are about 60 and 18 nm, respectively. These values are in excellent agreement with those reported earlier,[29,30,32] indicating that (i) the lamellae in each phase are virtually unaffected by those comprising the coexisting phase and (ii) SI/$(SI)_4$ mixing is, for the most part, minimal. In marked contrast, TEM and SAXS data obtained from immiscible diblock copolymer blends reveal that the α phase typically consists of 15−35% β, while the β phase is almost pure β.[26]

A series of digital TEM images showing the SI/$(SI)_4$ interface at different tilt angles between −45° and 30° in 15° increments is displayed in Figure 3. These images are all contrast-reversed to facilitate visualization of the alternating lamellae in each phase and identification of the colloidal gold beads (which appear as small bright dots). The SI/$(SI)_4$ interface is relatively sharp and is oriented almost parallel to the electron beam at $\theta = 0°$. As θ is increased or decreased substantially from 0°, the corresponding 2D TEM projections are seen to consist of superpositioned lamellae from each phase. In addition to being mass-normalized, these images have also been aligned with respect to the colloidal gold beads evident in the figure. The mean error σ incurred during alignment (averaged over all of the beads utilized) is shown as a function of θ in Figure 4, which reveals that, in 98% of the images, σ lies below the image resolution of 1 pixel. In fact, the overall σ averaged over the entire series of collected images is only 1.0 nm, as compared to the image sampling of 1.7 nm/pixel. Contributing to the alignment error is sample shrinkage induced by radiation damage under the electron beam. By comparing the positions of the colloidal gold beads before and immediately after collection of the tilt series, we estimate that the TEM specimen shrank laterally by about 1.8% during the course of image acquisition.

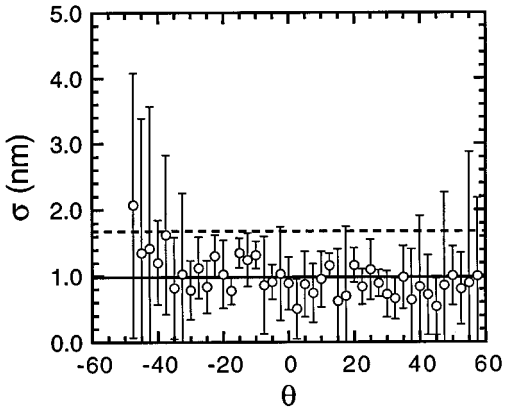

Figure 4. Mean alignment error (σ) as a function of tilt angle (θ). The vertical bars denote the standard deviation in σ, whereas the solid and dashed horizontal lines correspond to the overall mean σ (averaged over all θ) and the image resolution (per pixel).

Unlike model-dependent methods in which 2D TEM micrographs are compared to projections of a postulated structure of known symmetry,[42,43] electron tomography permits direct visualization of the complete 3D structure of an object *in situ*, reconstructed from a set of tilted views. Since this powerful method does not make any *a priori* assumptions or impose any requirements regarding the symmetry of the object, it has been proven

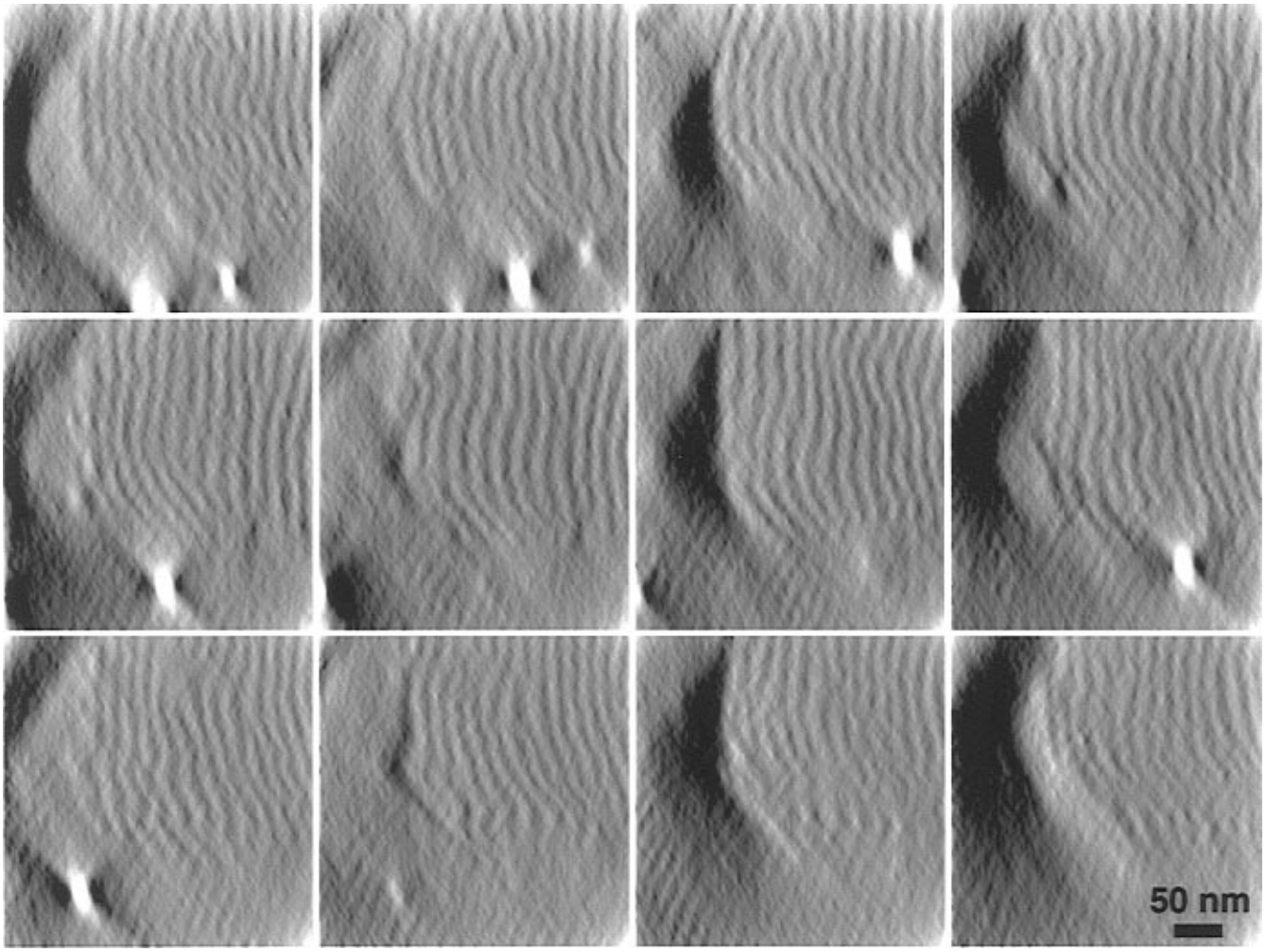

Figure 5. Slices of the reconstructed volume element generated from a complete series of tilt projections (6 out of 43 are shown in Figure 3) by the *r*-weighted (filtered) back-projection method. Each *xz* slice proceeds along the *y*-axis (perpendicular to the electron beam) from left to right and top to bottom. Bright dots correspond to colloidal gold beads.

to be extremely useful in the analysis of complex biological structures,[44−46] as well as of microphase-ordered block copolymers.[21,38] Two-dimensional (contrast-reversed) slices of the reconstructed volume element obtained from the complete series of 43 tilt projections are shown in Figures 5 and 6. Each slice is about 17 nm. To put this into proper perspective, a series of distortion-free sections of comparable thickness would be impossible to obtain by microtomy. While a solid reconstruction, in addition to or instead of the slices, could be provided here, it would not prove to be very beneficial due to the size difference between SI and $(SI)_4$ lamellae. The slices in Figure 5 are *xz* images displayed at different positions along the *y*-axis, where the *x*- and *y*-axes are normal to the electron beam and the *z*-axis is parallel to the electron beam. Large intermittent structures evident in the left portion of the images correspond to cross-sectioned lamellae in the SI phase, whereas the small lamellae evident in the slices are indicative of the $(SI)_4$ phase. Note that the $(SI)_4$ lamellae in this image series exhibit a $S_{1/2}$ disclination that clearly propagates away from the interface as the *y*-axis is traversed. The bright dot seen in one of the images once again identifies a dispersed colloidal gold bead and serves as an additional check on reconstruction accuracy; i.e., the better the reconstruction, the more circular the beads appear in cross section.

Images in Figure 6 are *xy* slices along the *z*-axis and clearly show the SI/$(SI)_4$ interface as in Figure 2. The difference between the images in Figures 2 and 6 is that the thin slices in Figure 6, containing less projected information and therefore exhibiting less interference, facilitate detailed visualization of interfacial features. In particular, the reader's attention is drawn to the points where the SI lamellae are physically connected to the adjacent $(SI)_4$ lamellae. While it is intuitively obvious that the lamellae from each phase must somehow be connected, no previous efforts have provided direct evidence for microphase connectivity (adhesion) in a copolymer/copolymer blend, especially at this spatial resolution. An understanding of such connectivity is vital to the design of multiphasic materials with interface-limited mechanical properties. As the *z*-axis is traversed, the images in Figure 6 reveal that SI/$(SI)_4$ lamellar adhesion can be lost and regained due to mismatch between the lamellar periodicities of the SI and $(SI)_4$ phases.

Thus far, only the interface separating the immiscible SI and $(SI)_4$ phases has been examined. In this section, we explore the morphologies that result when $(SI)_4$ molecules are trapped within the SI phase and when SI molecules reside in the $(SI)_4$ phase. As seen in the conventional TEM micrograph provided in Figure 7, the presence of short $(SI)_4$ molecules in the SI phase induces localized regions wherein the SI lamellae are highly frustrated, as evidenced by pinched lamellae and microstructural elements with nonzero curvature. To appreciate the influence of $(SI)_4$ midblock conformations

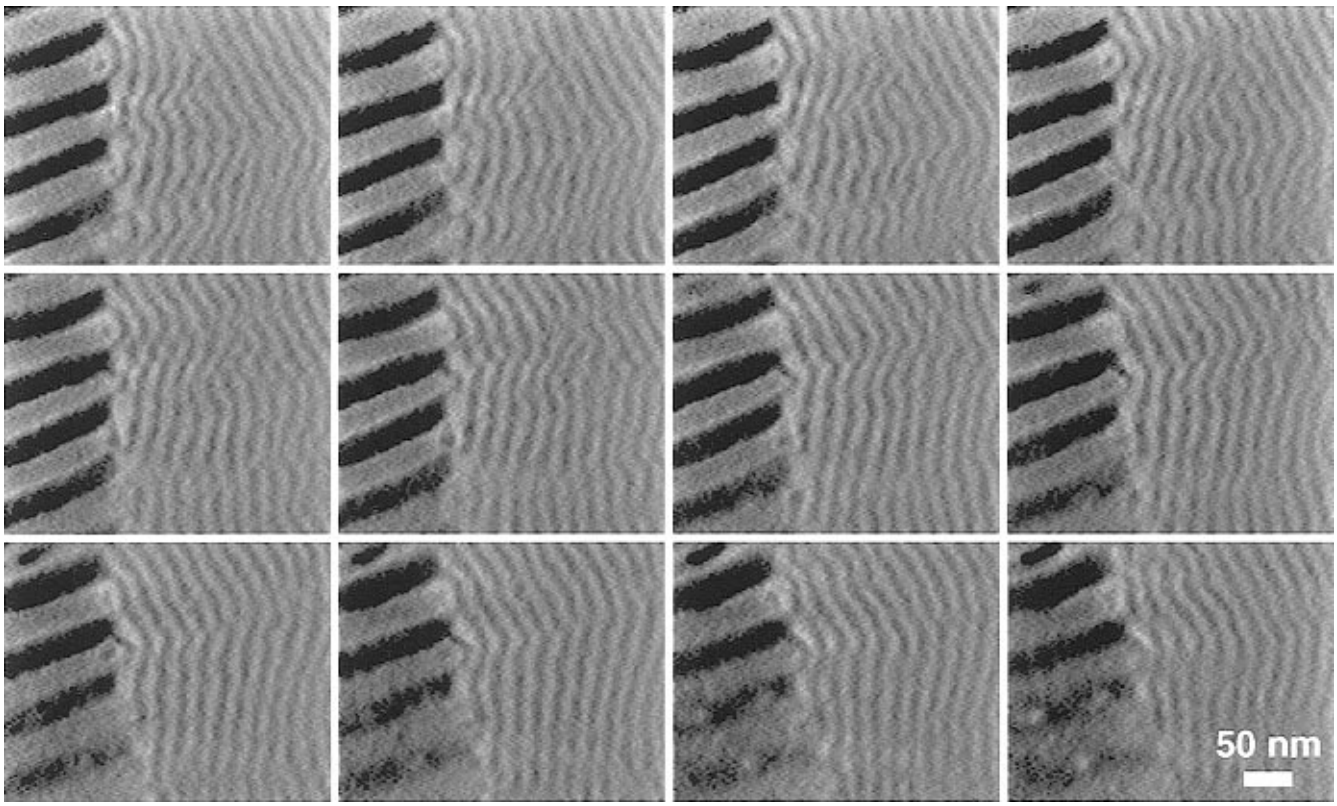

Figure 6. Series of sequential *xy* slices along the *z*-axis (parallel to the electron beam) from left to right and top to bottom. Each slice, measuring about 17 nm thick, reveals that the large lamellae of the SI copolymer adhere to the smaller lamellae of the $(SI)_4$ copolymer at discrete junction sites along the interface.

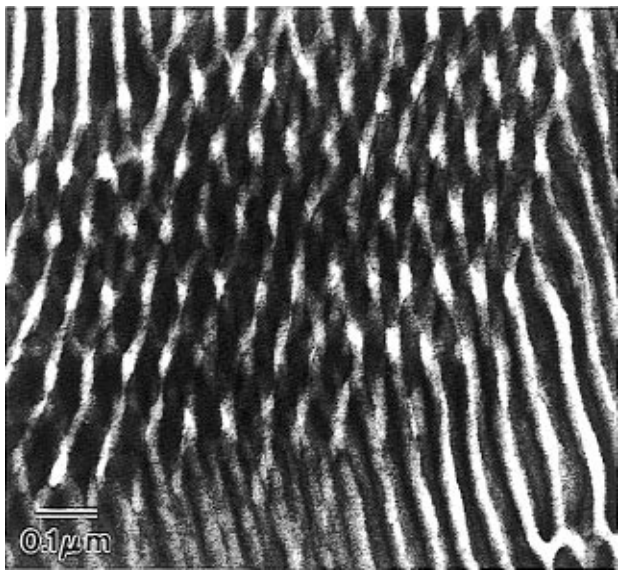

Figure 7. Conventional electron micrograph of an isolated region in the SI phase wherein $(SI)_4$ molecules have been trapped during macrophase separation. The presence of $(SI)_4$ molecules within SI lamellae serves to "pinch" the lamellae and consequently frustrate the local SI lamellar order, resulting in microdomain boundaries with nonzero mean curvature.

on SI conformations and lamellar microstructure, a schematic illustration of SI/$(SI)_4$ mixtures is presented in Figure 8. In the event that all of the $(SI)_4$ midblocks adopt a looped conformation (Figure 8a), the diblock/octablock blend is anticipated to behave as a blend of two diblock copolymers differing in block length by a factor of 8 (recall that a looped midblock is comparable to two single-grafted endblocks of half chain length). According to SCF predictions,[25] phase miscibility in such a diblock copolymer blend (with $\chi N_\alpha = 80$) is retained only up to about 27 vol % β copolymer. Figure 7 demonstrates, however, that innocuous incorporation of $(SI)_4$ molecules into the SI phase is not achieved. The frustrated lamellar morphology seen in this figure suggests that some of the $(SI)_4$ midblocks assume a bridged conformation, squeezing the longer SI molecules along the lamellar parallel (rather than allowing them to stretch along the lamellar normal) to satisfy the requirement of uniform density. Depending on the $(SI)_4$ midblock conformations in neighboring lamellae, squeezed SI molecules could conceivably induce a change in interfacial curvature (and in morphology) through chain packing considerations (see Figure 8b).

If SI molecules are trapped within the $(SI)_4$ phase during either micro- or macrophase separation, they could be similarly constrained, as seen by the SI inclusion in Figure 9. Rather than appearing as a multilamellar ("onion-skinned") vesicle, as block copolymers typically do when they macrophase-separate from, for example, a parent homopolymer of relatively high molecular weight, the SI inclusion seen here once again exhibits a frustrated lamellar-like morphology. Thus, the micrographs in Figures 7 and 9 indicate that, while the SI and $(SI)_4$ phases are almost completely demixed, isolated regions exist in each phase where the dissimilar copolymer molecules are forced to interact locally. In contrast, discrete homopolymer inclusions observed[34,47] in copolymer/homopolymer blends remain, for the most part, demixed due to strongly repulsive interactions between the homopolymer and the chemically dissimilar block of the copolymer. This is not, however, the case in the SI/$(SI)_4$ blend in which the macromolecules comprising the inclusions and matrix are compositionally identical and are both capable of self-assembling into ordered microstructures to minimize the magnitude of unfavorable interactions between covalently linked

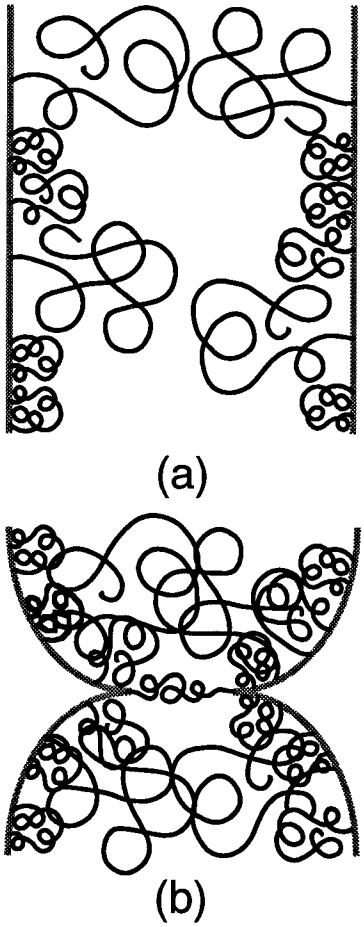

Figure 8. Illustration of SI and $(SI)_4$ copolymer molecules residing in the same microdomain. In (a), the $(SI)_4$ molecules adopt a completely looped conformation so that the blend can be envisioned as a diblock copolymer/copolymer blend in which the block length ratio is 8:1 SI:$(SI)_4$. If the midblocks of the $(SI)_4$ molecules assume a bridged conformation, they constrain and squeeze the longer SI blocks, as in (b).

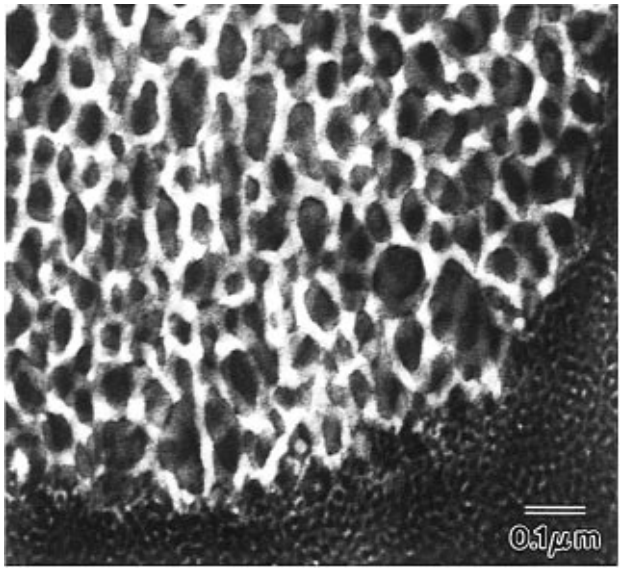

Figure 9. Electron micrograph of an SI copolymer inclusion residing in the $(SI)_4$ matrix. The nonlamellar SI morphology evident here is indicative of mixing between SI and $(SI)_4$ molecules within the inclusion.

blocks. This shared characteristic of the SI and $(SI)_4$ copolymer molecules therefore is responsible for limited intramicrodomain mixing, while the architecture of the $(SI)_4$ copolymer is responsible for SI microdomain frustration, within the isolated regions seen in Figures 7 and 9.

Conclusions

An equimolar blend of a diblock copolymer and an octablock copolymer, both of identical composition and molecular weight, is found to be immiscible. Electron micrographs show that the blend exhibits clearly defined macroscopic interfaces, as well as isolated (and highly frustrated) inclusions of one copolymer within a matrix of the other. In addition, electron tomography has been employed to explore the features of the blend interface at relatively high resolution (ca. 3 nm). Slices parallel and perpendicular to the interface reveal that (i) the octablock phase in close proximity to the interface comprises defects (due to periodicity mismatch) that propagate normal to the interface and (ii) adhesion between the diblock and octablock phases is a result of discretely connected lamellae. These results demonstrate that electron tomography can provide heretofore unavailable adhesion information from interfaces and could be of tremendous value in the study of related structural characteristics, e.g., grain boundaries,[48] in ordered block copolymer systems. Comparison of the morphological features observed here with experimental data[26] and theoretical predictions[25] reported for immiscible diblock copolymer blends suggests that the molecular architecture and midblock conformations of the octablock copolymer are responsible for diblock/octablock blend immiscibility. With this observation in mind, block architecture and conformation should be considered carefully as a design criterion in technological applications employing multiblock copolymers and their blends.

Acknowledgment. This work has been supported by the National Science Foundation (CMS-941-2361) and the Director, Office of Energy Research, Office of Basic Energy Sciences, Materials Science Division of the U.S. Department of Energy, under contract DE-AC03-76SF00098. One of us (R.J.S.) thanks the National Center for Electron Microscopy for a Visiting Scientist Fellowship and Drs. K. M. Krishnan and U. Dahmen for valuable discussions. Funding for D.A.A., J.W.S., M.B.B., and J.C.F. was provided by the Howard Hughes Medical Institute and the National Institutes of Health (GM31627, D.A.A.; GM25101, J.W.S.). We are grateful to Mr. H. Chen (UCSF) for valuable technical assistance.

References and Notes

(1) Leibler, L. *Macromolecules* **1980**, *13*, 1602.
(2) Legge, N. R.; Holden, G.; Schroeder, H. E., Eds. *Thermoplastic Elastomers: A Comprehensive Review*; Hanser: New York, 1987.
(3) Fredrickson, G. H.; Bates, F. S. *Annu. Rev. Phys. Chem.* **1990**, *41*, 525.
(4) Binder, K. *Phys. Scr.* **1994**, *55*, 206.
(5) Almdal, K.; Koppi, K. A.; Bates, F. S.; Mortensen, K. *Macromolecules* **1992**, *25*, 1743.
(6) Hajduk, D. A.; Gruner, S. M.; Rangarajan, P.; Register, R. A.; Fetters, L. J.; Honeker, C.; Albalak, R. J.; Thomas, E. L. *Macromolecules* **1994**, *27*, 490.
(7) Jackson, C. L.; Barnes, K. A.; Morrison, F. A.; Mays, J. W.; Nakatani, A. I.; Han, C. C. *Macromolecules* **1995**, *28*, 713.
(8) Albalak, R. J.; Thomas, E. L. *J. Polym. Sci., Polym. Phys. Ed.* **1993**, *31*, 37; **1994**, *32*, 341.
(9) Scott, D. B.; Waddon, A. J.; Lin, Y. G.; Karasz, F. E.; Winter, H. H. *Macromolecules* **1992**, *25*, 4175.
(10) Winey, K. I.; Patel, S. S.; Larson, R. G.; Watanabe, H. *Macromolecules* **1993**, *26*, 2542.
(11) Winey, K. I.; Thomas, E. L.; Fetters, L. J. *Macromolecules* **1991**, *24*, 6182.

(12) Tanaka, H.; Hasegawa, H.; Hashimoto, T. *Macromolecules* **1991**, *24*, 240. Kimishima, K.; Hashimoto, T.; Han, C. C. *Macromolecules* **1995**, *28*, 3842.
(13) Winey, K. I.; Thomas, E. L.; Fetters, L. J. *J. Chem. Phys.* **1991**, *95*, 9367.
(14) Winey, K. I.; Thomas, E. L.; Fetters, L. J. *Macromolecules* **1992**, *25*, 422, 2645.
(15) Spontak, R. J.; Smith, S. D.; Ashraf, A. *Macromolecules* **1993**, *26*, 956.
(16) Disko, M. M.; Liang, K. S.; Behal, S. K.; Roe, R.-J.; Jeon, K. J. *Macromolecules* **1993**, *26*, 2983.
(17) Matsen, M. W. *Phys. Rev. Lett.* **1995**, *74*, 4225. Matsen, M. W. *Macromolecules* **1995**, *28*, 5765.
(18) Hadziioannou, G.; Skoulios, A. *Macromolecules* **1982**, *15*, 267.
(19) Zhao, J.; Majumdar, B.; Schulz, M. F.; Bates, F. S.; Almdal, K.; Mortensen, K.; Hajduk, D. A.; Gruner, S. M. *Macromolecules*, in press.
(20) Vilesov, A. D.; Floudas, G.; Pakula, T.; Melenevskaya, E. Yu.; Birshtein, T. M.; Lyatskaya, Yu. V. *Macromol. Chem. Phys.* **1994**, *195*, 2317.
(21) Spontak, R. J.; Fung, J. C.; Braunfeld, M. B.; Sedat, J. W.; Agard, D. A.; Kane, L.; Smith, S. D.; Satkowski, M. M.; Ashraf, A.; Hajduk, D. A.; Gruner, S. M. *Macromolecules*, submitted.
(22) Mayes, A. M.; Russell, T. P.; Deline, V. R.; Satija, S. K.; Majkrzak, C. F. *Macromolecules* **1994**, *27*, 7447.
(23) Shi, A.-C.; Noolandi, J.; Hoffmann, H. *Macromolecules* **1994**, *27*, 6661. Shi, A.-C.; Noolandi, J. *Macromolecules* **1994**, *27*, 2936.
(24) Spontak, R. J. *Macromolecules* **1994**, *27*, 6363.
(25) Matsen, M. W. *J. Chem. Phys.* **1995**, *103*, 3268.
(26) Hashimoto, T.; Yamasaki, K.; Koizumi, S.; Hasegawa, H. *Macromolecules* **1993**, *26*, 2895. Hashimoto, T.; Koizumi, S.; Hasegawa, H. *Macromolecules* **1994**, *27*, 1562.
(27) Matsen, M. W.; Bates, F. S. *Macromolecules* **1995**, *28*, 7298.
(28) Milner, S. T.; Witten, T. A.; Cates, M. E. *Macromolecules* **1989**, *22*, 853.
(29) Spontak, R. J.; Smith, S. D.; Satkowski, M. M.; Ashraf, A.; Zielinski, J. M.; In *Polymer Solutions, Blends, and Interfaces*; Noda, I., Rubingh, D. N., Eds.; Elsevier: Amsterdam, 1992.
(30) Smith, S. D.; Spontak, R. J.; Satkowski, M. M.; Ashraf, A.; Lin, J. S. *Phys. Rev. B* **1993**, *47*, 14555.
(31) Matsushita, Y.; Mogi, Y.; Mukai, H.; Watanabe, J.; Noda, I. *Polymer* **1994**, *35*, 246.
(32) Smith, S. D.; Spontak, R. J.; Satkowski, M. M.; Ashraf, A.; Heape, A. K.; Lin, J. S. *Polymer* **1994**, *36*, 4527.
(33) Matsen, M. W. *J. Chem. Phys.* **1995**, *102*, 3884.
(34) Spontak, R. J.; Smith, S. D.; Ashraf, A. *Macromolecules* **1993**, *26*, 5118.
(35) Hong, S.-U.; Duda, J. L.; Smith, S. D.; Hajduk, D. A.; Spontak, R. J. *Macromolecules*, manuscript in preparation.
(36) Frank, J., Ed. *Electron Tomography: Three-Dimensional Imaging with the Transmission Electron Microscope*; Plenum: New York, 1992.
(37) Bates, R. H. T.; McDonnell, M. J. *Image Restoration and Reconstruction*; Clarendon: Oxford, UK, 1986.
(38) Spontak, R. J.; Williams, M. C.; Agard, D. A. *Polymer* **1988**, *29*, 387.
(39) Fung, J. C.; Liu, W.; deRuijter, W. J.; Chen, H.; Abbey, C. K.; Sedat, J. W.; Agard, D. A. *J. Struct. Biol.*, in press.
(40) Chen, H.; Swedlow, J. R.; Grote, M.; Sedat, J. W.; Agard, D. A. In *Handbook of Biological Confocal Microscopy*; Pawley, J. B., Ed.; Plenum Press: New York, 1995.
(41) Kane, L.; Smith, S. D.; Satkowski, M. M.; Ashraf, A.; Spontak, R. J. Presented at the Intersociety Polymer Conference, Baltimore, MD, October 1995. Kane, L. M.S. Thesis, North Carolina State University, in progress.
(42) Anderson, D. M.; Bellare, J.; Hoffman, J. T.; Hoffman, D.; Gunther, J.; Thomas, E. L. *J. Colloid Interface Sci.* **1992**, *148*, 398.
(43) Burger, C.; Antonietti, M.; Ruland, W. *J. Chem. Phys.*, submitted.
(44) McEwen, B. F.; Arena, J. J.; Frank, J.; Rieder, C. L. *J. Cell Biol.* **1993**, *120*, 301.
(45) Horowitz, R. A.; Agard, D. A.; Sedat, J. W.; Woodcock, C. L. *J. Cell Biol.* **1994**, *125*, 1.
(46) Moritz, M.; Braunfeld, M. B.; Fung, J. C.; Sedat, J. W.; Alberts, B. M.; Agard, D. A. *J. Cell Biol.* **1995**, *130*, 1149.
(47) Pan, T.; Huang, K.; Balazs, A. C.; Kunz, M. S.; Mayes, A. M.; Russell, T. P. *Macromolecules* **1993**, *26*, 2860.
(48) Gido, S. P.; Gunther, J.; Thomas, E. L.; Hoffman, D. *Macromolecules* **1993**, *26*, 4506. Gido, S. P.; Thomas, E. L. *Macromolecules* **1994**, *27*, 849, 6137.

MA9515691